

Compositional Optimization of Amyloid-Graphene Oxide Nanohybrids for Biomaterials

A Senior Project presented to the Faculty of the Materials Engineering Department,
California Polytechnic State University, San Luis Obispo

In Partial Fulfillment of the Requirements for the Degree Bachelor of Science

By

Claire Drewery

Under the advisement of Trevor S. Harding Ph.D and Shanju Zhang Ph.D

June 2019

Abstract

Amyloid nanofibrils are natural materials capable of self-assembling into precise structures with tunable functionalities, while exhibiting excellent mechanical properties. In combination with highly conductive graphene oxide (GO), the 1-D amyloid nanofibrils and 2-D nanosheets of GO can produce a robust and bio-functional nanohybrid, hypothesized to exhibit multi-domain functional properties useful for enzyme sensing, water purification, drug delivery, and tissue scaffolding applications. Here, we examine the properties of an amyloid-graphene oxide nanohybrid film made with amyloids derived from hen egg white lysozymes in an attempt to explore the diverse toolbox of amyloid derivatives and establish ideal fabrication methods and formulations of maximization of biofunctionality. Ideal methods for producing a stable and robust nanohybrid material will result in exfoliation of graphene oxide with the adherence of dispersed amyloid fibril structures between planes. In this study XRD is utilized to determine if exfoliation is achieved across varied film compositions. AFM, POM, FTIR and DSC were utilized to confirm successful formation of amyloids and graphene oxide and examine thermal property effects across varied compositions. Results from XRD tests suggested intercalation rather than exfoliation was achieved, and that increasing the weight percentage of amyloids correlated to an increase in the inter-sheet spacing between graphene oxide planes. From DSC tests, an irreversible stress relaxation effect was observed due to residual stress from film casting.

Keywords: Amyloids, Graphene Oxide, Nanohybrid, X-Ray Diffraction, Materials Engineering, Biofunctionality, Biomaterials, Differential Scanning Calorimeter, Atomic Force Microscopy, Fourier Transform Infrared Spectroscopy, Nanocomposite, Biosensors, Water filtration, Drug Delivery, Tissue Engineering

Acknowledgements

I would like to acknowledge my project advisor, Dr. Trevor Harding of the Cal Poly Materials Engineering Department, as well as my technical advisor, Dr. Shanju Zhang of the Cal Poly Chemistry and Biochemistry Department, for all of their help and guidance throughout the course of this project. Within the Cal Poly Chemistry and Biochemistry Department, I would like to thank Fangyou Xie for his aid in the synthesis of the components in this project and training on the Fourier Transform Infrared spectrometer, as well as Denzel Ayala for his help regarding Atomic Force Microscopy. I would also like to thank technician, Eric Beaton of the Materials Engineering Department, who provided me with training on the Differential Scanning Calorimeter. Lastly, I would like to thank the National Science Foundation for providing the financial support for this project.

Table of Contents

<i>Abstract</i>	<i>i</i>
<i>Acknowledgements</i>	<i>ii</i>
<i>List of Figures</i>	<i>v</i>
<i>List of Tables</i>	<i>vi</i>
<i>List of Abbreviations</i>	<i>vii</i>
1 Introduction	1
1.1. Background	1
1.2 Review of Literature	1
1.2.1 Bio-Nanohybrid Materials	1
1.2.2 Amyloid-Graphene Oxide Nanohybrid	2
1.2.3 Intercalation of Graphene Oxide	3
1.2.4 Studies on Methods of Intercalation	4
1.3 Proposed Research	5
2 Materials and Methods	6
2.1 Materials	6
2.2 Synthesis of Graphene Oxide	6
2.2.1 Expansion of Graphene	6
2.2.2 Pre-Oxidation of Graphene	7
2.2.3 Oxidation of Graphene	7
2.2.4 Collection of Graphene Oxide	7
2.3 Synthesis of Amyloids	7
2.4 Preparation of Films	7
2.5 Characterization of Nanohybrid and Components	8
2.5.1 Microscopy	8
2.5.2 FTIR Chemical Analysis	8
2.5.3 XRD Structural Analysis	8
2.5.4 DSC Thermal Analysis	9
3 Results and Discussion	10
3.1 Formation of Components	10
3.1.1 Graphene Oxide	10
3.1.2 Amyloids	11
3.2 Bond Mobility	12
3.3 Interlayer Spacing	13
3.4 Thermal Observations	14
4 Conclusions	15
Appendix A	16

<i>Appendix B</i>	<i>17</i>
<i>Appendix C</i>	<i>18</i>
<i>References</i>	<i>19</i>

List of Figures

FIGURE 1.1: Supramolecular self-assembly of b-lactoglobulin into amyloid fibrils.

FIGURE 1.2: The structure of Graphene-Oxide 2-D sheets

FIGURE 1.3: Nanoscale structure consisting of black graphene oxide sheets and blue amyloid fibrils in an (a) separated, (b) intercalated and (c) exfoliated structure.

FIGURE 2.1: (a) Films A, B and C drop cast onto a Teflon surface and (b) covered with an aerated cover.

FIGURE 3.1: POM image of the edge of nanohybrid film showing layers of GO.

FIGURE 3.2: FTIR spectrum from 0.6 wt % GO with characteristic peaks.

FIGURE 3.3: 1 μm^2 area AFM image from cast 3 wt % amyloid solution depicting nanofibers.

FIGURE 3.4: FTIR of 3 wt % amyloid solution showing characteristic peaks.

FIGURE 3.5: XRD spectra with GO peak from 14 wt % amyloid film.

FIGURE 3.6: Linear trend of d-spacing from XRD results of each film composition.

FIGURE 3.7: DSC heat-cool-heat-cool cycle from 25-200°C of 12 wt % film.

List of Tables

TABLE 2.1: Components of GO and Amyloid Synthesis Solutions

TABLE 3.1: Comparison of % Transmission of Significant Peaks Found in FTIR of Films

List of Abbreviations

GO	G raphene O xide
HEWL	H en E gg W hite L ysozymes
TGA	T hermogravimetric A nalysis
FTIR	F ourier T ransform I nfrared S pectroscopy
DSC	D ifferential S canning C alorimeter
XRD	X - R ay D iffractometer
AFM	A tomistic F orce M icroscopy
wt %	W eight percent

Chapter 1

Introduction

1.1. Background

Amyloid-graphene oxide nanohybrids are a composite material made of 1-D amyloid nanofibrils and 2-D nanosheets of graphene oxide. Amyloid nanofibrils are a self-assembled structure derived from proteins, which exhibit high tensile strength and a functionality that facilitates interaction or combination of target molecules with the fibrils. Graphene oxide also possesses high tensile strength, as well as high conductivity. Through integration, the nanohybrid offers an action-response functionality, in which the levels of interaction of the amyloids with target molecules triggers a corresponding response in the conductivity of the graphene oxide. This functionality is useful for several biomaterial applications including use in biosensors, drug delivery, water purification and tissue engineering. Previous research has in fact proven amyloid-graphene oxide nanohybrids to be a promising biosensor material, with enzyme sensing abilities.

In order to achieve maximum functionality as a biomaterial for these applications, good dispersion of the amyloids within the sheets of the graphene oxide must be achieved in the nanohybrid. There are three levels of dispersion possible with graphene oxide, the first and least dispersed being a separated dispersion; the next dispersion level being intercalated, followed by exfoliated.

1.2 Review of Literature

1.2.1 *Bio-Nanohybrid Materials*

Molecular or polymeric species derived from biological origins, prepared in combination with inorganic materials, both in the nanometric scale, form the basis of a bio-nanohybrid material. The development of these materials emerged in the early 2000's [1]. Because of the versatility of bio-nanohybrid materials in their applications, great interest has been drawn to the subject and the modes of functional properties which can be derived. The combination of inorganic nanomaterials with biological materials has also brought to light interdisciplinary work between Life Sciences and Materials Sciences and Nanotechnology. Differences in chemical composition and structure determine the properties exhibited by the given bio-nanohybrid and its functionality. Intents for such nanohybrids include mimicking natural materials with improvements in properties as well as functionalizing for regenerative, biosensing and drug delivery applications.

1.2.2 Amyloid-Graphene Oxide Nanohybrid

Amyloid-graphene nanohybrids are a novel class of bio-nanohybrids consisting of 1-D self-assembled protein nanofibers and 2-D graphene-oxide nanosheets.

1.2.3.1 Amyloids

Amyloids have gained recent attention due to their self-assembling nature and potential as a building block for biosensors. Beta sheets of amino acids stack together in aggregates to form long insoluble fibers (Fig. 1.1) when thermodynamically favorable, which are insoluble [2]. Aggregated amyloids were thought to be harmful within the body as they were discovered to contribute to the onset of Alzheimer's in the form of insoluble amyloid beta 42 protein fragments [3]. However, research into the manipulation of amyloids and incorporation of amyloids into nanocomposites has established their advantageous properties as a stabilizer and structural component. Functionalized amyloids have been synthesized using specific proteins chosen for fibril formation that may act as a bioreceptor, which can be manipulated to target a specific enzyme or bind to the analyte molecules to monitor activity of a specific reaction [4].

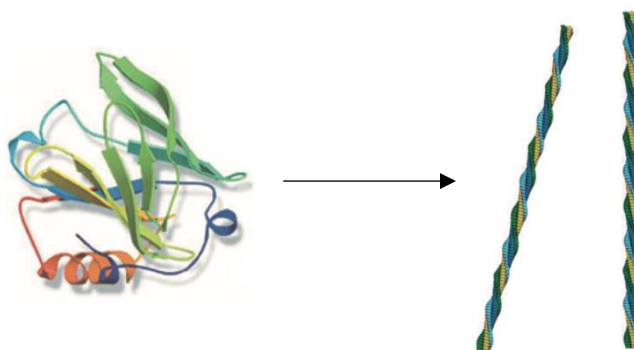


FIGURE 1.1: Supramolecular self-assembly of b-lactoglobulin into amyloid fibrils. Image adapted from Li, Chaoxu, *et al.* [5].

1.2.3.2 Graphene Oxide

Graphene oxide (GO) consists of a hexagonal carbon lattice containing several chemical impurities such as hydroxyl, carbonyl and sulfate groups (Fig. 1.2) which demonstrate considerable effects on its properties [6].

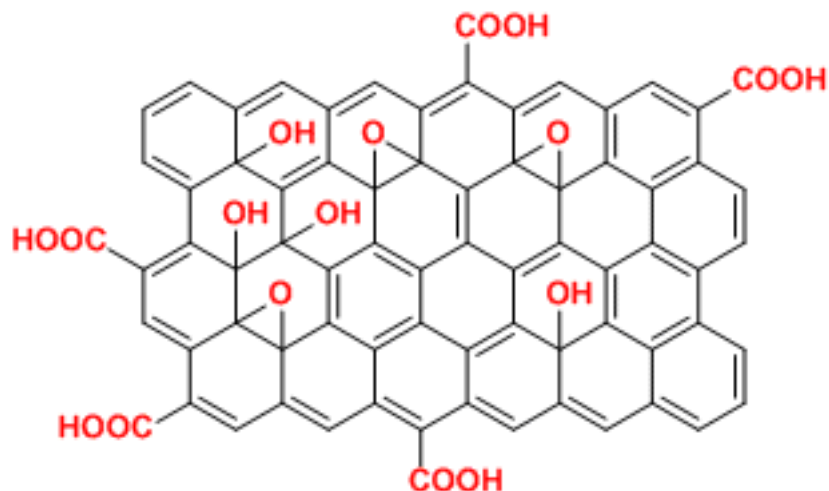


FIGURE 1.2: The structure of Graphene-Oxide 2-D sheets

The extent of these impurities is derived from the processing methods used. Hummer's method is a simplified, safe, quick and efficient method, which obtains GO through treatment of graphite with sulfuric acid and potassium permanganate. GO may be reduced into a pure graphene structure; however, characterization of exfoliated GO sheets has shown to exhibit larger intercalation spacing which may be advantageous for production of a well dispersed polymer nanocomposite. Presence of functional groups in GO also enables easier coupling interactions between the filler and the matrix [7]. Bulk material of dispersed GO sheets is termed graphene oxide.

1.2.3.3 Composite Properties

Tensile properties of amyloid-graphene nanocomposite films have been characterized using various ratios of graphene-amyloid composition in a study conducted by C. Li, J. Adamcik and R. Mezzenga [5]. Tensile strength of the films was found to be between 6-18 MPa with tensile moduli between ~ 2.5 to 8.0 GPa. Maximum tensile properties were found at a composition of 1:2, with increasing amounts of amyloids tending to decrease tensile properties. Increasing amyloid composition was thought to be due to presence of amyloids not adsorbed on to the graphene surfaces. Maximum electrical conductivity of $5.1 \times 10^{-1} \text{ S cm}^{-1}$ was found at 1:0.5 composition and was four orders of magnitude greater than that of a pure GO film. Conductivity of 1:2 composition was lower, however still vastly greater than pure GO.

1.2.3 Intercalation of Graphene Oxide

In general, increases in nanocomposite mechanical properties can be attributed to uniform dispersion of the nanofiller within the matrix; therefore, it is essential for the amyloid-graphene nanocomposite to achieve an ideally intercalated structure in order to produce a film with good mechanical properties. Intercalation

is the process of insertion of a molecule into a material with a layered structure. In this case, intercalation of amyloids into GO sheets (Fig. 1.3).

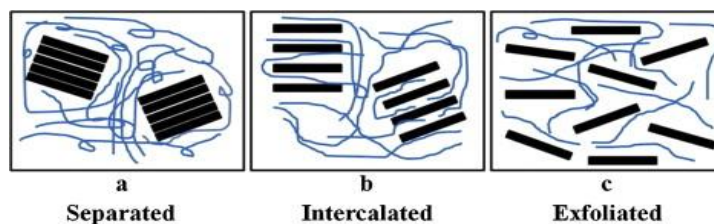


FIGURE 1.3: Nanoscale structure consisting of black graphene oxide sheets and blue amyloid fibrils in an (a) separated, (b) intercalated and (c) exfoliated structure.

Production of nanocomposites with GO-derived fillers hinges largely on the exfoliation of GO before incorporation into the polymer matrix [8]. Exfoliation of GO is the manipulation of graphene sheets to increase interlayer spacing and alter orientation. Increasing the interlayer spacing of the sheets will allow incorporation of the amyloid fibrils between the sheets of graphene in order to maximize interaction and adhesion of the amyloid and graphene surfaces. Fully exfoliated graphene oxide, with amyloid fibrils dispersed between the sheets, will produce the best mechanical and biosensing properties as the interactions with the amyloid fibrils will be able to easily cause a response in the GO sheets as well as hold the structure together.

1.2.3.1 *Measuring Intercalation*

Intercalation of amyloids into the graphene may be measured through observation of interlayer distance of the graphene using XRD imaging or SAXS as well as observation of fibril attachment onto graphene surfaces using TEM or SEM imaging.

1.2.4 *Studies on Methods of Intercalation*

1.2.4.1 *Composition*

Composition has been seen to play a role in the dispersion of amyloids on surfaces of GO and the resulting composite properties. In C. Li, J. Adamcik and R. Mezzenga [5] investigation of the graphene-amyloid ratio concluded that an optimal ratio of 1:2 resulted in maximum mechanical properties. Increasing the amyloid concentration was determined to decrease mechanical properties due to unattached fibrils.

1.2.4.1 *Sonication*

Sonication time was investigated in S. Ye and J. Feng [9] as a factor of mechanical exfoliation for pure GO films and their resulting mechanical properties. Maximum mechanical properties were observed at continual sonication time of 2 minutes at 100 W and 40 kHz. Increasing sonication time was determined to gradually cause fragmentation and defects of the GO sheets.

1.3 Proposed Research

In order for amyloid-graphene oxide nanohybrids to maximize functionality for biomaterial applications, intercalation or exfoliation of the amyloids within the graphene oxide must be achieved.

The scope of this project extends to the synthesis of amyloid and graphene oxide components as well as the fabrication of an amyloid-graphene oxide nanohybrid films in varying compositions. A minimum of achieving intercalation of the two components of the film is attempted as an exfoliated structure is difficult to achieve and characterize. Studies of the film and individual components were performed to confirm successful synthesis of each component and nanohybrid as well as determine the interlayer spacing of the graphene oxide.

Chapter 2

Materials and Methods

2.1 Materials

The materials used in this project for expansion and oxidation of graphene include graphite flakes, sulfuric acid (H_2SO_4), nitric acid (HNO_3), potassium persulfate ($\text{K}_2\text{S}_2\text{O}_8$), potassium permanganate (KMnO_4), phosphorus pentoxide (P_2O_5), hydrogen peroxide (H_2O_2), and deionized (DI) water. Materials used for synthesis of amyloids include hen egg white lysozymes (HEWL), and hydrochloric acid (HCl). Total amounts of each material used are listed in Table 2.1. All chemicals were used as-received unless dilutions are noted.

TABLE 2.1: Components of GO and Amyloid Synthesis Solutions

	Component	Amount
Graphene Oxide	Graphite flakes	5 g
	H_2SO_4	650 mL
	HNO_3	50 mL
	DI water	approx. 5 L
	$\text{K}_2\text{S}_2\text{O}_8$	4.2 g
	P_2O_5	6.2 g
	KMnO_4	15 g
	30 % H_2O_2	10 mL
Amyloids	HEWL	0.6 g
	1 M HCl	19.4 g

Equipment such as an oven, furnace, hot oil baths, ice baths, an aspirator pump with 0.2 μm filter, p-8 filter paper and a centrifuge were needed for synthesis of graphene oxide. An oven was also needed for synthesis of amyloids. The solutions were placed in a bath sonicator at 40°C for 5 minutes following mixing of GO and amyloids. For drop casting of the films, a Teflon surface and aerated cover was used.

2.2 Synthesis of Graphene Oxide

Synthesis of GO consists of 4 steps: expansion of graphene, pre-oxidation of graphene, oxidation of graphene and collection of graphene oxide.

2.2.1 Expansion of Graphene

Expansion of graphene was performed with the starting material, graphite flakes, mixed into a solution of 150 mL sulfuric acid and 50 mL of nitric acid. This solution was stirred for 24 hours, followed by quenching

with 700 mL of DI water. Using an aspirator pump and 0.2 μm filter, the solution was washed with DI water until the solution had a pH of 4. The solution was dried in an oven at 50°C for 24 hours, then separated into crucibles, which were placed in an oven at 1000°C for 45 minutes then cooled.

2.2.2 Pre-Oxidation of Graphene

The pre-oxidation step was performed using 5 g of the expanded graphene resulting from the previous step, in a solution of 300 mL sulfuric acid, 4.2 g potassium persulfate, and 6.2 g of phosphorus pentoxide. This solution was stirred for 5 hours in a hot oil bath at 80°C and cooled. The solution was then quenched with 700 mL of DI water. The solids were separated with an aspirator pump and 0.2 μm filter until a pH of 4 was reached, then dried.

2.2.3 Oxidation of Graphene

Oxidation of the graphene was completed using 5 g of the resulting pre-oxidized graphene mixed into a solution of 200 mL sulfuric acid in an agitated ice bath. 15 g of potassium permanganate was slowly added into the solution, which was then transferred into a hot oil bath at 40°C and stirred at 200 rpm for 3 hours. 1700 mL of DI water was added to dilute the solution, and hydrogen peroxide was added to stop the oxidation process.

2.2.4 Collection of Graphene Oxide

The resulting solution was centrifuged a total of 19 times using a JA-20 centrifuge at 20,000 rpm and 5°C for 30 minutes; 3 initial times using DI water, once with 1 M HCl, a following 14 times with DI water and once with DI water and the resulting solution after filtering through p-8 filter paper. The solution was analyzed using TGA to determine a weight percent of 0.79 wt% GO, then diluted to 0.6 wt % with DI water for ease of film preparation purposes.

2.3 Synthesis of Amyloids

A 20 g solution of 3 wt % HEWL starting protein in 1M hydrochloric acid was mixed and heated in an oven at 60 °C for 5 days. The resulting solution increased in opacity and viscosity.

2.4 Preparation of Films

The 3 wt % amyloid solution was diluted with DI water to bring its pH up and prepare 10 g solutions of ratios of 1:5, 1:6 and 1:7 with the 0.6 wt % GO solution. Each drop was labeled film A, B and C for the 1:5, 1:6 and 1:7 ratio solutions, respectively for casting (Fig 2.1a). Each solution was drop cast onto a Teflon surface using a pipette, avoiding addition of air. Each drop was covered with an aerated cover (Fig. 2.1b)

to slow evaporation rate until films were dry. This resulted in films with compositions of 17, 14 and 12 wt % amyloids.

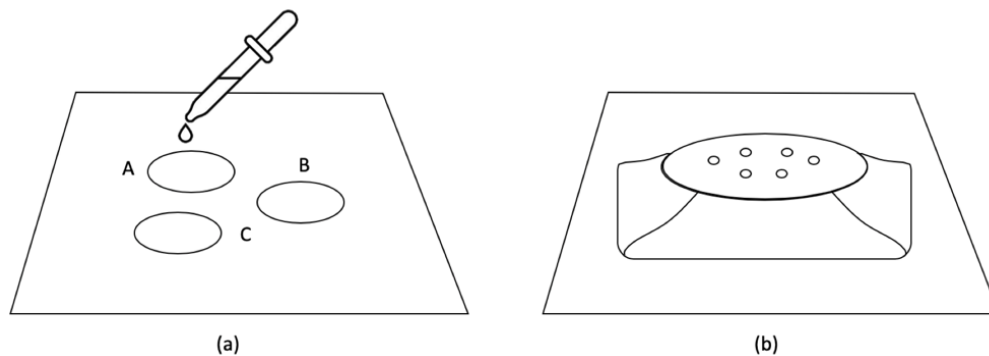


FIGURE 2.1: (a) Films A, B and C drop cast onto a Teflon surface and (b) covered with an aerated cover.

2.5 Characterization of Nanohybrid and Components

2.5.1 Microscopy

Two methods of microscopy were used for identification of components and confirmation of successful formation of amyloids and GO: Atomic Force Microscopy (AFM) and Polarized Optical Microscopy (POM). The 3 wt % amyloid solution was cast onto a sanitized microscope slide for AFM imaging. Images of the amyloids were taken using an MRP-3D AFM head and AC160TS tip in tapping mode, with a 1 μm scan size, 1.5 Hz scan rate and 512 points and lines resolution. POM images of a nanohybrid film were taken using a Leica 2700 microscope in transmission mode using a λ lens filter.

2.5.2 FTIR Chemical Analysis

To determine the functional groups, analyze bond mobility and validate the chemical composition of the components and films, FTIR analysis was performed on the 3 wt % amyloid solution, 0.6 wt % GO solution and each dry film composition. Using a Thermo Fisher Nicolet IS10, spectra were taken from 400 to 4000 cm^{-1} at 1.0 cm^{-1} resolution.

2.5.3 XRD Structural Analysis

To characterize the atomic structure of each of the dry film compositions, X-Ray Diffractometry was conducted using a Siemens Diffraktometer D5000 run from 2θ of 3 to 40° at on each dry film composition with a 0.01° step at a rate of $1^\circ/\text{min}$ and max of 40 kV and 40 mA. Tests were conducted using a scattering vector window of 2 nm^{-1} and Cu $K\alpha$ radiation ($\lambda = 0.154 \text{ nm}$). According to Bragg's Law, decreasing θ of a diffraction peak, means higher d-spacing, or spacing between regular atomic planes (Eqn. 2.1). In this case regular atomic planes of graphene oxide within the films are analyzed to determine the interlayer

spacing using XRD. Theoretically, increasing the interlayer spacing of the graphene oxide should mean that amyloids are interacting with the planes and ideally intercalating between the nanosheets.

$$2d \sin \theta = \lambda \quad (\text{Equation 2.1})$$

2.5.4 DSC Thermal Analysis

To determine thermal properties of each dry film composition, Differential Scanning Calorimetry was performed using a Mettler Toledo DSC 3+ using heat-cool-heat-cool cycling from 25-200°C at 10°C/min. Tests were carried out using covered aluminum sample holders containing 2.5 ± 0.2 mg specimens.

Chapter 3

Results and Discussion

3.1 Formation of Components

3.1.1 Graphene Oxide

The semi-crystalline layers of graphene oxide at the edge of a nanohybrid film can be seen in images on a polarized optical microscope (POM). This image is consistent with results from previous studies [5], suggesting successful synthesis of the nanohybrid films and graphene oxide.

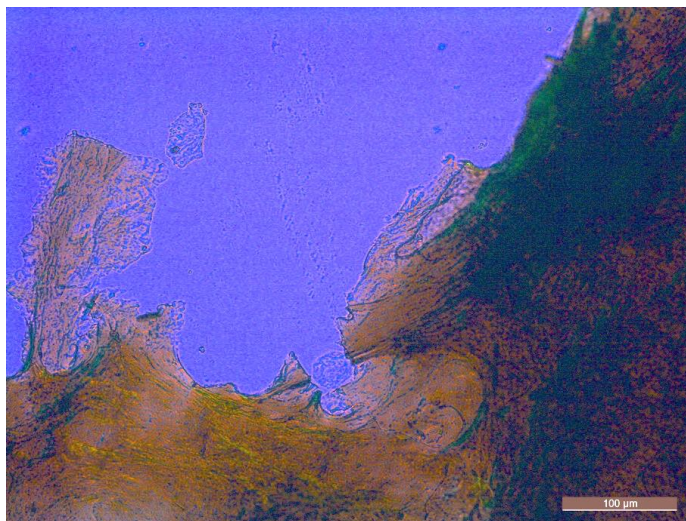


FIGURE 3.1: POM image of the edge of nanohybrid film showing layers of GO.

Characteristic peaks from the FTIR spectra of the 0.6 wt% solution of GO include a peak at 3409.84 cm^{-1} , which indicates stretching of intermolecular hydrogen bonds, 2362.91 and 2084.73 cm^{-1} , which suggests the presence of carbonyl groups, 1630.03 cm^{-1} , which suggests the presence of C=C aromatic rings, and 1044.60 cm^{-1} , which indicates stretching of C-OH. These significant peaks are in agreement with studies done by T. Rattana, S. Chaiyakuna, *et al.* [10] on characterization of graphene oxide nanosheets.

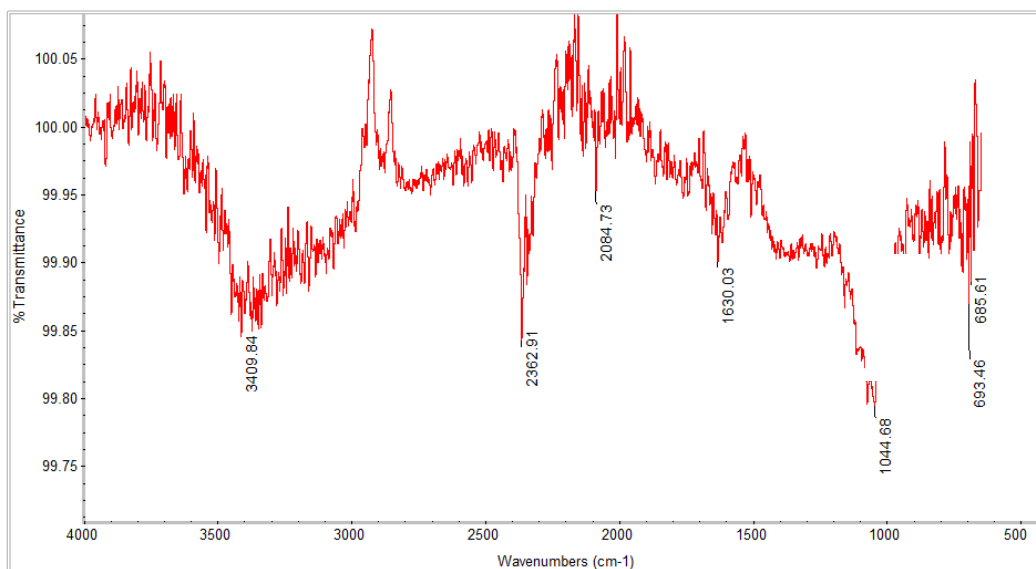


FIGURE 3.2: FTIR spectrum from 0.6 wt % GO with characteristic peaks.

3.1.2 Amyloids

Nanofibers ~ 5 nm in thickness were apparent in AFM images. Due to flaws in the flatness of the glass slide surface used to cast the 3 wt % amyloid solution, images were not as clear as in previous studies using cleaved mica. A study by L. Arnaudov and R. Vries [11] on amyloid fibers derived from HEWL found that a procedure similar to the one used in this study was optimal for forming fibers, and synthesized fibers ~ 4 nm in thickness, also determined through AFM imaging.

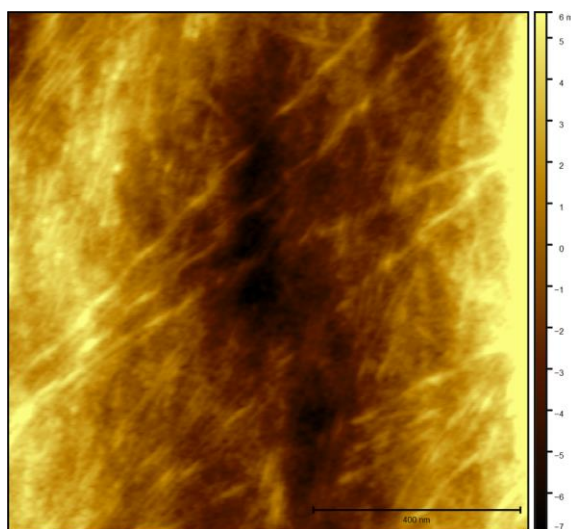


FIGURE 3.3: 1 μm^2 area AFM image from cast 3 wt % amyloid solution depicting nanofibers.

Characteristic peaks of the amyloids from the FTIR spectra of the 3 wt % amyloid solution included peaks at 1652.08 and 1540.58 cm^{-1} , indicating presence of C=O functional groups, as well as at 1239.78 cm^{-1}

indicating presence of C-O-C acetate bonds. These three peaks were similar to significant peaks found in the fibril ATR-FTIR spectra in C. Li *et al.* [5].

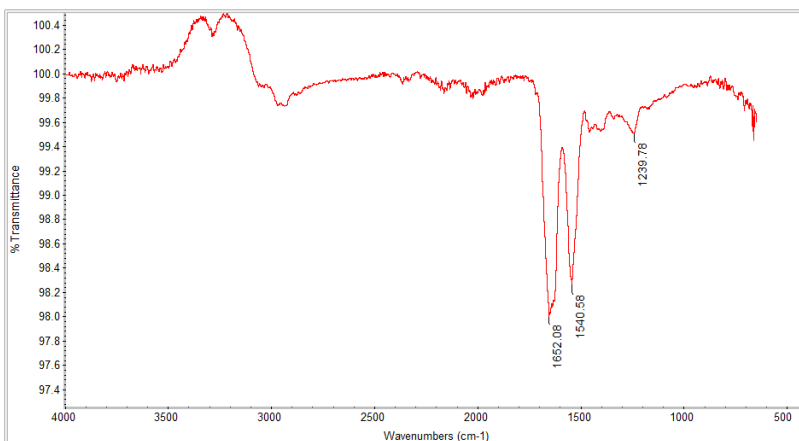


FIGURE 3.4: FTIR of 3 wt % amyloid solution showing characteristic peaks.

3.2 Bond Mobility

Changes in bond mobility with composition of the dry films was examined through comparisons of FTIR spectra. Individual spectra of each film composition are detailed in Appendix A. From a table specifying the intensity of % Transmission of the similar peaks found in the film spectra (Table 2) it can be found that of the two films with 17 and 14 wt % amyloid composition, higher % Transmission values were observed over those values of the 12 wt % amyloid composition film. With increase in % transmission, there is less absorbance of the IR wave by the chemical bonds of the specimen. Therefore, bond mobility was observed to decrease with an increase in % wt amyloid composition of the films. This may be due to increases in the interaction or intermolecular bonding between graphene oxide and amyloids from improvements in intercalation.

TABLE 3.1: Comparison of % Transmission of Significant Peaks Found in FTIR of Films

Wavenumber (cm ⁻¹)	Composition (wt % Amyloids)		
	17	14	12
1055	85.0	85.2	84.0
1224	89.1	89.3	88.1
1427	92.3	92.7	92.0
1561	90.1	90.3	89.1
1869	95.6	95.4	94.3
2573	93.8	94.0	92.6

3.3 Interlayer Spacing

For each nanohybrid film composition, a peak at $2\theta \sim 9.9^\circ$ was observed (Fig 3.5). The peak angle was found to decrease with increasing wt % of amyloids, suggesting that with increasing wt % amyloids, there is an increase in interlayer spacing between graphene oxide planes (Fig. 3.6). Increasing interlayer spacing means amyloids are moving between the planes of the graphene oxide, and intercalation is improving. Individual graphs of the XRD run for each composition are detailed in Appendix B. According to studies by K. Krishnamoorthy *et al.* [12] pure graphene oxide diffraction peaks like at $2\theta \sim 10.91\text{-}10.12^\circ$. A slight increase in the d-spacing of pure graphene oxide was observed with incorporation of amyloids. However, not enough to indicate the amyloid fibrils have moved between the planes of GO.

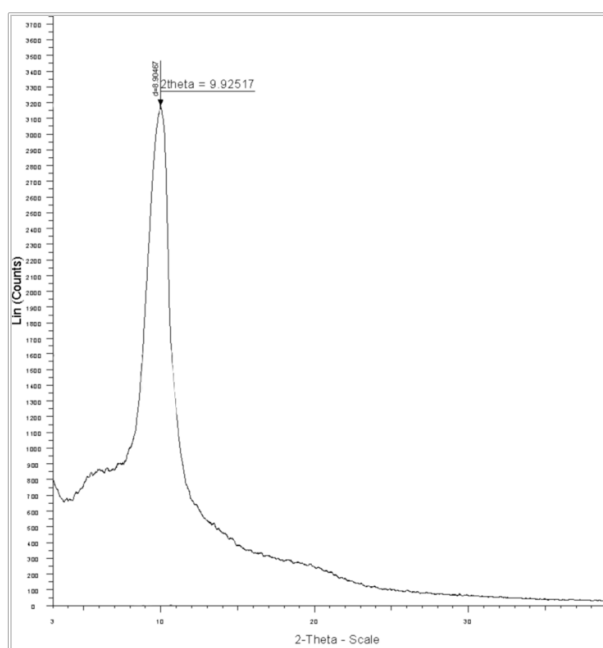


FIGURE 3.5: XRD spectra with GO peak from 14 wt % amyloid film.

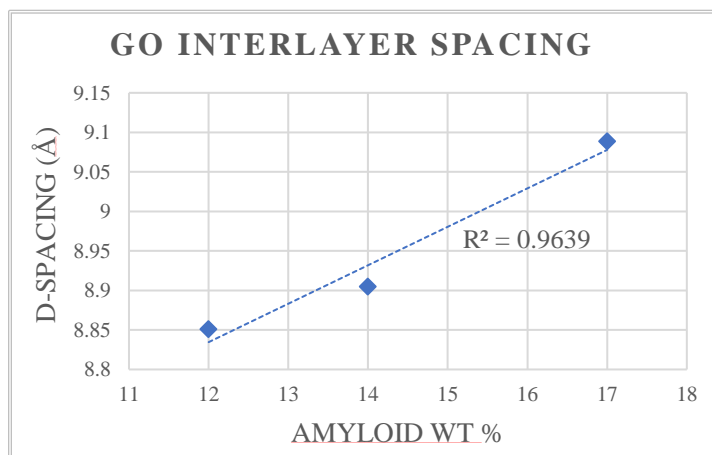


FIGURE 3.6: Linear trend of d-spacing from XRD results of each film composition.

3.4 Thermal Observations

On the first heat cycle of DSC testing, a dip in the heat flux was observed (Fig 3.7). Upon the second heating cycle, this feature was not reproduced. This thermal phenomenon was observed across DSC testing of each film composition. It was hypothesized that this event may be due to stress relaxation, caused by residual stresses formed within the film during the evaporation process of casting. Similar casting processes performed in J. Cheung *et al.* [13] found residual stresses in film formation caused by restriction of polymer chains.

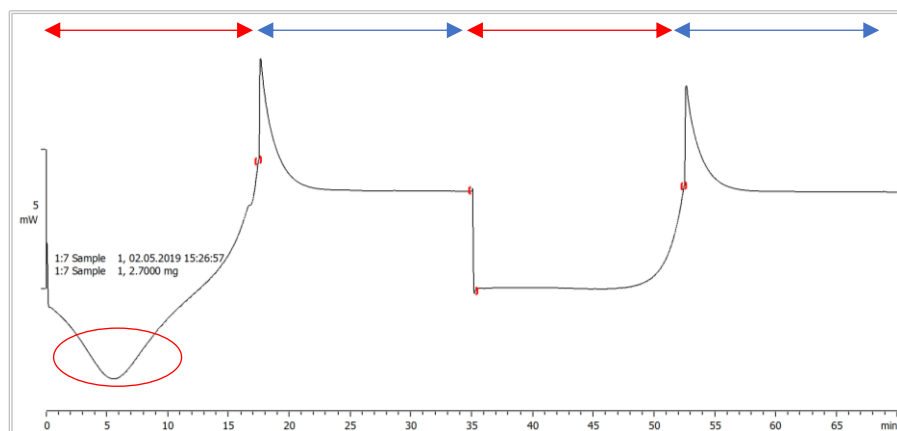


FIGURE 3.7: DSC heat-cool-heat-cool cycle from 25-200°C of 12 wt % film.

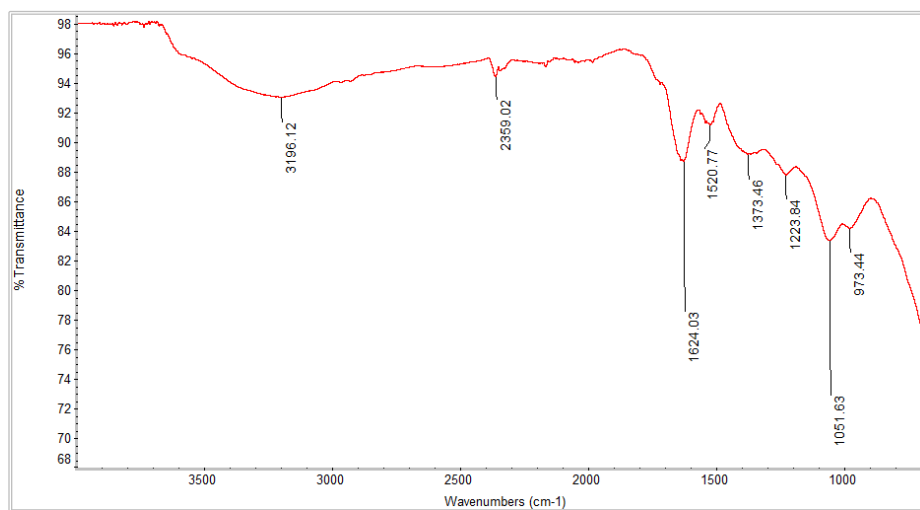
Chapter 4

Conclusions

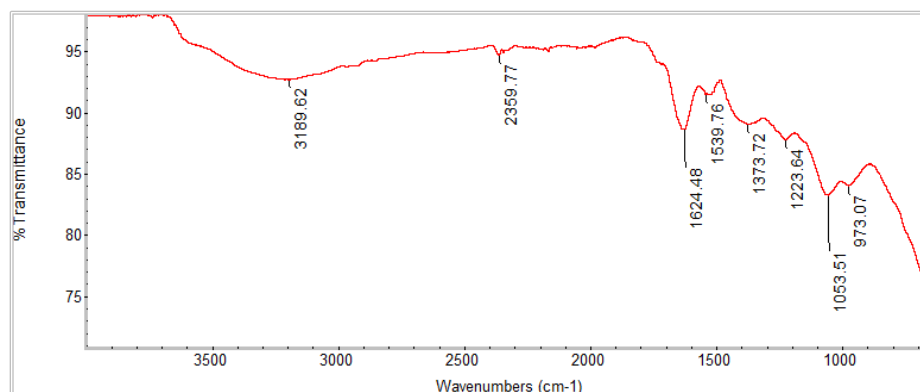
1. Increasing weight percent of amyloids increases the interlayer spacing between graphene oxide nanosheets.
2. Increasing weight percent of amyloids limits bond mobility of graphene oxide and amyloid components.
3. Stress relaxation of the nanohybrid films occurs upon first heat cycle between 25-100°C due to residual stresses from casting.

Appendix A

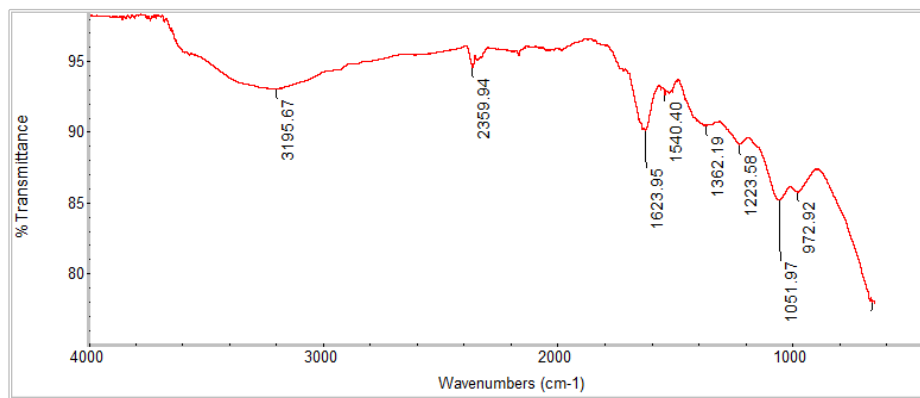
FTIR Spectra



17 wt % Amyloid Film



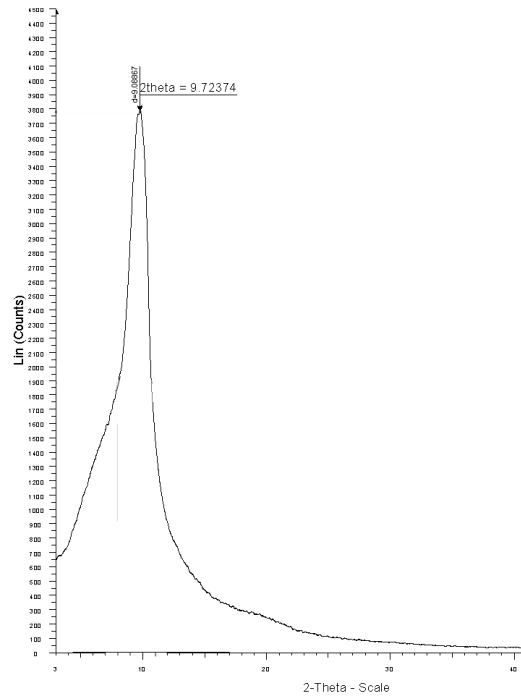
14 wt % Amyloid Film



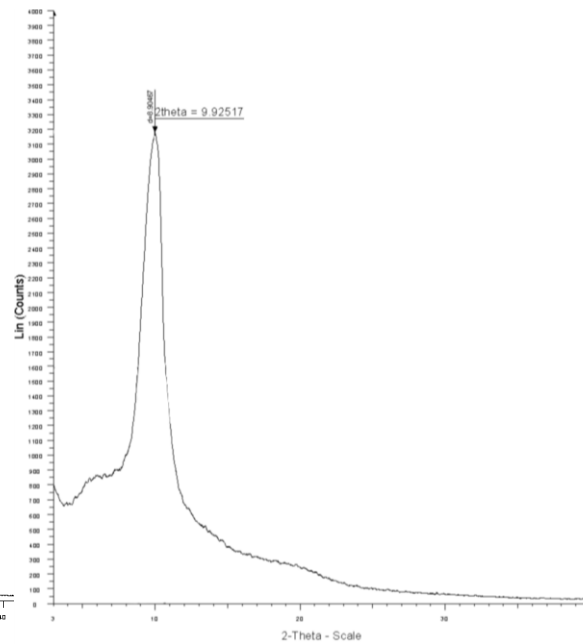
12 wt % Amyloid Film

Appendix B

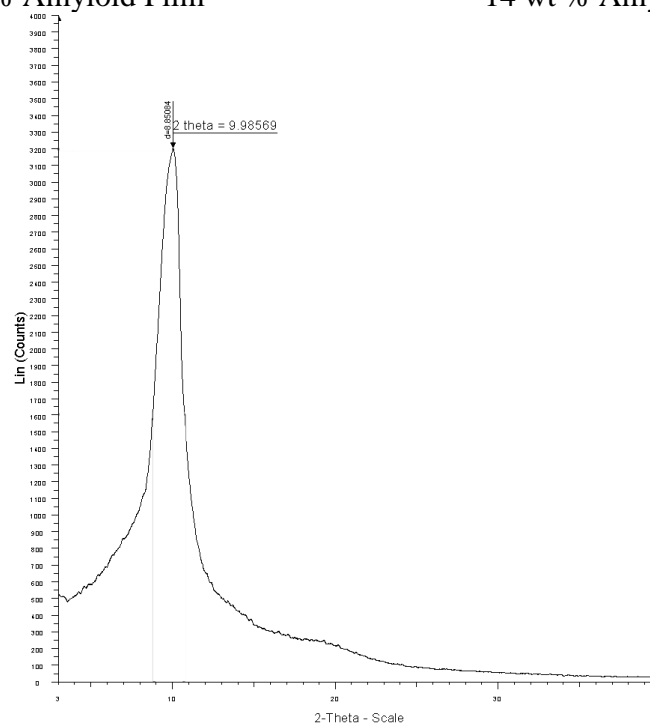
XRD Spectra



17 wt % Amyloid Film



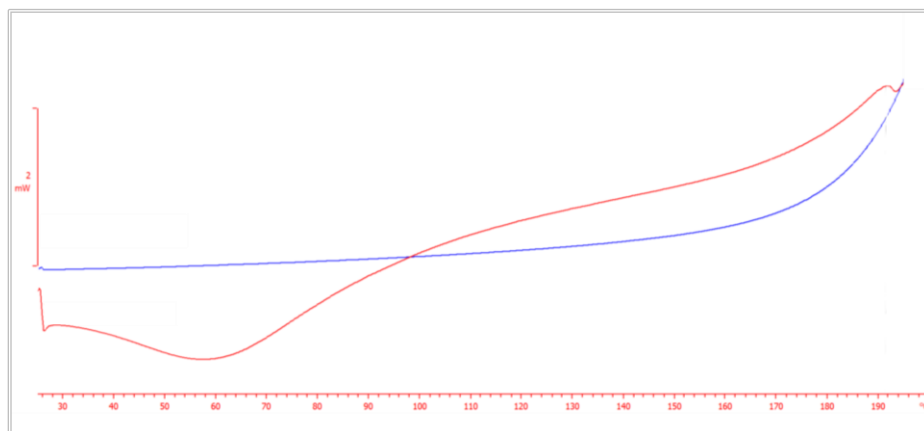
14 wt % Amyloid Film



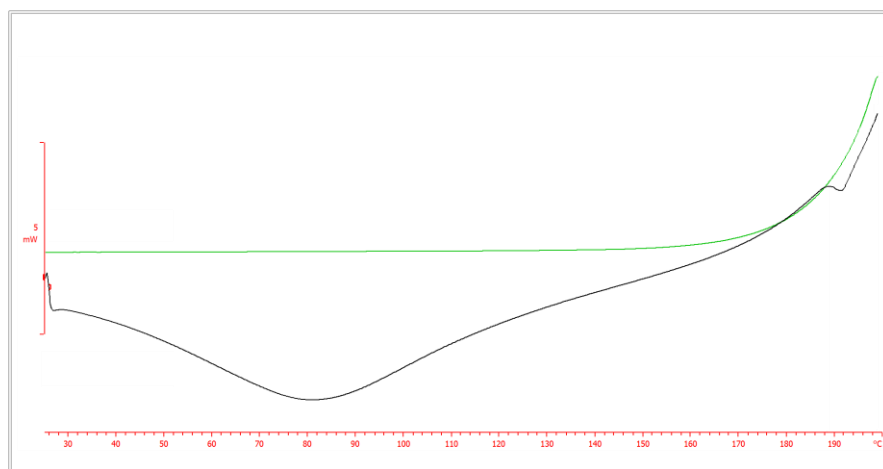
12 wt % Amyloid Film

Appendix C

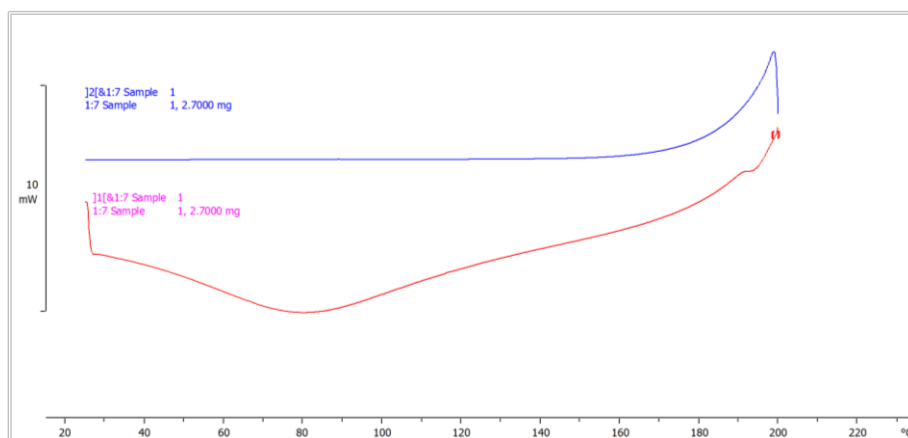
DSC Curves



17 wt % Amyloid Film



14 wt % Amyloid Film



12 wt % Amyloid Film

References

- [1] E. Ruiz-Hitzky, P. Aranda and M. Darder, "An Introduction to Bio-nanohybrid Materials," in *Bio-inorganic Hybrid Nanomaterials*, WILEY, 2008, pp. 1-2.
- [2] J. Castillo-León, K. B. Andersen and W. E. Svendsen, "Self-Assembled Peptide Nanostructures for Biomedical Applications: Advantages and Challenges," in *Biomaterials Science and Engineering*, InTech, 2001, pp. 115-138.
- [3] "Amyloid," Wikipedia, [Online]. Available: en.wikipedia.org/wiki/Amyloid.
- [4] S. Mankar, A. Anoop, S. Sen and S. K. Maji, "Nanomaterials: amyloids reflect their brighter side," *Nano Reviews*, vol. 2, 2011.
- [5] C. Li, J. Adamcik and R. Mezzenga, "Biodegradable nanocomposites of amyloid fibrils and graphene with shape-memory and enzyme-sensing properties," *Nature Nanotechnology*, vol. 7, p. 421–427, 2012.
- [6] "Graphite Oxide," Wikipedia, [Online]. Available: en.wikipedia.org/wiki/Graphite_oxide.
- [7] R. K. Layek and A. K. Nandi, "A review on synthesis and properties of polymer functionalized graphene," *Polymer*, vol. 54, no. 19, pp. 5087-5103, 2013.
- [8] J. R. Potts, D. R. Dreyer, C. W. Bielawski and R. S. Ruoff, "Graphene-based polymer nanocomposites," *Polymer*, vol. 52, no. 1, pp. 5-25, 2011.
- [9] S. Ye and J. Feng, "The effect of sonication treatment of graphene oxide on the mechanical properties of the assembled films," *RSC Advances*, no. 46, pp. 39681-39687, 2016.
- [10] T. Rattana, S. Chaiyakuna, N. Witit-anun, N. Nuntawong, P. Chindaudom, S. Oaew, C. Kedkeaw and P. Limsuwan, "Preparation and characterization of graphene oxide nanosheets," *Procedia Engineering*, vol. 32, p. 759 – 764, 2012.
- [11] L. N. Arnaudov and R. Vries, "Thermally Induced Fibrillar Aggregation of Hen Egg White Lysozyme," *Biophysical Journal*, vol. 88, no. 1, pp. 515-526, 2005.
- [12] K. Krishnamoorthy, M. Veerapandian, K. Yun and S.-J. Kim, "The chemical and structural analysis of graphene oxide with different degrees of oxidation," *Carbon*, vol. 53, pp. 38-49, 2013.
- [13] J. Y. Chung, T. Q. Chastek, M. J. Fasolka, H. W. Ro and C. M. Stafford, "Quantifying Residual Stress in Nanoscale Thin Polymer Films via Surface Wrinkling," *ACS Nano*, vol. 3, no. 4, pp. 844-852, 2009.